ADVANCES IN ATMOSPHERIC SCIENCES, VOL. 25, NO. 1, 2008, 96–??

A Scheme for Estimating Tropical Cyclone Intensity Using AMSU-A Data

YAO Zhigang*[1] (姚志刚), LIN Longfu[2] (林龙福), CHEN Hongbin[1] (陈洪滨), and FEI Jianfang[3] (费建芳)

[1] *Laboratory for Middle Atmosphere and Global Environment Observation, Institute of Atmospheric Physics, Chinese Academy of Sciences, Beijing* 100029

[2] *Beijing Institute of Applied Meteorology, Beijing* 100029

[3] *Institute of Meteorology, PLA University of Science and Technology, Nanjing* 211101

(Received 6 November 2006; revised 30 April 2007)

ABSTRACT

Brightness temperature anomalies measured by the Advanced Microwave Sounding Unit (AMSU) on the National Oceanic and Atmospheric Administration (NOAA) polar-orbiting series are suited to estimate tropical cyclone (TC) intensity by virtue of their ability to assess changes in tropospheric warm core structure in the presence of clouds. Analysis of the measurements from different satellites shows that the variable horizontal resolution of the instrument has significant effects on the observed brightness temperature anomalies. With the aim to decrease these effects on TC intensity estimation more easily and effectively, a new simple correction algorithm, which is related to the product of the brightness temperature gradient near the TC center and the size of the field-of-view (FOV) observing the TC center, is proposed to modify the observed anomalies. Without other measurements, the comparison shows that the performance of the new algorithm is better than that of the traditional, physically-based algorithm. Furthermore, based on the correction algorithm, a new scheme, in which the brightness temperature anomalies at 31.4 GHz and 89 GHz accounting for precipitation effects are directly used as the predictors with those at 54.94 GHz and 55.5 GHz, is developed to estimate TC intensity in the western North Pacific basin. The collocated AMSU-A observations from NOAA-16 with the best track (BT) intensity data from the Japan Meteorological Agency (JMA) in 2002–2003 and in 2004 are used respectively to develop and validate regression coefficients. For the independent validation dataset, the scheme yields 8.4 hPa of the root mean square error and 6.6 hPa of the mean absolute error. For the 81 collocated cases in the western North Pacific basin and for the 24 collocated cases in the Atlantic basin, compared to the BT data, the standard deviations of the estimation differences of the results are 15% and 11% less than those of the CIMSS (Cooperative Institute for Meteorological Satellite Studies, University of Wisconsin-Madison) TC intensity AMSU estimation products.

Key words: AMSU, brightness temperature anomalies, tropical cyclone, minimum sea level pressure

DOI: 10.1007/s00376-008-0096-3

1. Introduction

Accurate assessment of initial intensity is an important component of short-term tropical cyclone (TC) intensity forecasts. In the past nearly thirty years, some studies (**??**; **?**; **?**; **?**; **?**; **?**; **?**; **?**; **?**) have been conducted to estimate TC intensities from passive microwave radiometer data. Although TC centers are usually masked by a dense cirrus canopy, it is almost transparent for microwave radiances. Through thermodynamic and dynamic constraints on the TC scale, measurements (55 GHz region) of TC upper-tropospheric warm anomalies are correlated with minimum sea level pressure (MSLP).

As stated by **?**, the hydrodynamic equation cannot be applied directly to obtain the sea level pressure due to the scattering by large particles

*Corresponding author: YAO Zhigang, zhigangyao@mail.iap.ac.cn

Table 1. AMSU-A radiometer characteristics.

Channel No.	Frequency (GHz)	Weighting function peak
1	23.8	Surface
2	31.4	Surface
3	50.3	Surface
4	52.8	900 hPa
5	53.596	600 hPa
6	54.4	400 hPa
7	54.94	250 hPa
8	55.5	150 hPa
9	v_1=57.290344	90 hPa
10	v_1±0.217	50 hPa
11	v_1±0.3222±0.022	25 hPa
12	v_1±0.3222±0.022	10 hPa
13	v_1±0.3222±0.010	5 hPa
14	v_1±0.03222±0.0045	2.5 hPa
15	89.0	Surface

and the coarse horizontal resolution of current microwave temperature sounding instruments, which causes them to sub-sample the relatively small TC warm core. The above effects can be accounted for implicitly using regression analysis. If a set of pairs of warm anomaly observations from a satellite-borne radiometer and almost contemporary *in situ* observations of sea level pressure deficit are available, a statistical relationship can be fitted and subsequently used to estimate pressure deficits from satellite observations. **?** and **?** have applied this approach to National Oceanic and Atmospheric Administration (NOAA) series MSU (Microwave Sounding Unit) observations for the Atlantic and western North Pacific TC basins.

The Advanced MSU (AMSU) flies aboard NOAA satellites 15, 16, 17, and 18. AMSU is a cross-track scanning radiometer and measures at 20 discrete frequencies. It consists of two instruments, named AMSU-A and AMSU-B. AMSU-A (see Table 1) is primarily for providing temperature soundings, but it is also useful in deriving other TC parameters, including cloud liquid water and rain rate. AMSU-B is primarily for providing moisture soundings. For more details of the AMSU instruments and TC applications, see Kidder et al. (2000).

Although the horizontal resolution of AMSU-A has been improved significantly compared to its predecessors, it cannot fully resolve the maximum warming, which is concentrated in the eye of a TC and occupies an average diameter of about 50 km (**?**). In order to decrease the effects of a coarse and varying resolution of the same or different microwave instruments on observations, **?** first introduced a physically-based scheme to retrieve the warm anomalies of a TC. Similarly, **?** developed a TC estimation algorithm that uses 55-GHz AMSU data to estimate MSLP. Their method includes a correction for sub-sampled upper-tropospheric warm anomalies (UTWA) that uses AMSU-B data to estimate eye size. However, their retrievals are sensitive to the eye-size parameter, which may not be accurate enough. **?** statistically related six AMSU-derived parameters to the maximum winds of Atlantic TCs. Their results, reported as the average error standard deviation, corresponded closely with reconnaissance data (9.1 kn) but degraded markedly (14.6 kn) for cases without aircraft observations. **?** developed a TC intensity estimation algorithm, which depends on 18 parameters derived from AMSU data and one additional non-AMSU-derived parameter available in real time. Recently, for taking into account the effects of scattering by large particles, **?** developed an empirical correction algorithm using 31.4 GHz (Ch2) and 89 GHz (Ch15) for the Atlantic basin. However, the correction and regression equations are valid only for subsequent cases drawn from the same population as their dependent data. Wacker's equations are therefore not generally applicable to other regions of the world, where the distribution of TC size and intensity may differ.

With the aim to decrease the effects of varying horizontal resolution of AMSU-A on observations of brightness temperature (T_{B}) anomalies more easily and effectively, a new algorithm is proposed to modify the observed T_{B} anomalies. Furthermore, to take into account the effects of precipitation on estimation, the T_{B} anomalies at 31.4 GHz and 89 GHz are used directly as the predictors with those at 54.94 GHz (Ch7) and 55.5 GHz (Ch8) in the estimation algorithm. As far as the authors are aware, most previous studies about AMSU TC intensity estimation have focused on cases in the Atlantic. In this study, attention is paid to cases in the western North Pacific basin, where TCs are most active in the globe. The collocated AMSU-A observations from NOAA-16 with the best track (BT) intensity data from the Japan Meteorological Agency (JMA) in 2002–2003 and in 2004 are used respectively to train and validate regression coefficients. Additionally, data from 2003–2004 in the Atlantic basin are used to further evaluate the constructed regression algorithm. Finally, the results are compared with operational AMSU TC intensity estimation products.

2. Data

The datasets utilized in this study consist of AMSU observations and post-analyzed BT data. AMSU-A data are provided by the NOAA/National Environmental Satellite, Data, and Information Service (NESDIS). Generally, the reconnaissance data are consid-

ered as "ground truth". While they are unavailable, the BT intensity data are the best alternative for developing and validating the intensity estimation algorithm, as in the studies carried out by **?**, **?**, and **?**. The intensities of the post-analyzed BT data are determined from available aircraft reconnaissance measurements (nearly all of which are from the Atlantic), drifting buoys, ship reports, land stations, satellite cloud-track winds, Dvorak satellite estimates, and scatterometer and passive microwave (SSM/I) surface winds. In this study, AMSU-A observations are collocated with BT data obtained from the RSMC (Regional Specialized Meteorological Centre) Tokyo-Typhoon Center/JMA from 2002–2004 in the western North Pacific basin. The collocating criteria and steps are based on the following: (1) the BT data are linearly interpolated to the time of the most recent AMSU data; (2) the nearest field-of-view (FOV) to the position obtained from the BT data is selected; (3) for the 55.5-GHz channel, the warmest one of the four FOVs around the selected FOV is considered as the FOV observing the TC center; (4) compute the environmental T_{B} using the selected two FOVs spaced $+/-$ 10 FOVs in the along-track direction from the FOV being considered above; and (5) the cases for which the warmest FOVs of the 54.94-GHz channel and 55.5-GHz channel are different are excluded. One of the advantages of step (4) is to avoid the effects of non-systematic biases in the cross-track direction on T_{B} anomalies. These biases may be different for the same kind of instrument onboard different satellites. By including this step, when the measured anomalies are used in the intensity estimation, it is not necessary to remove spot-to-spot systematic biases caused by asymmetry of the observations, even for AMSU-A on different satellites. A second advantage is that environmental T_{B}'s can be determined in the same track data for each case, even in which the TC center is far from the nadir position. Furthermore, step (5) is added for removing the abnormal cases in which the warm structure of the TC is not in the vertical direction, which can cause the warmest FOVs for the 54.94- and 55.5-GHz channels to be different. The current methods do not focus on dealing with the above abnormal structure.

There are 573 collocated cases available, including 344 in 2002–2003 and 229 in 2004. In the following study, in order to evaluate objectively the regression equations, the former dataset is used to obtain the multi-linear regression coefficients and the latter is applied to evaluate the constructed estimation equations. A histogram of cases for the dependent and independent dataset is shown in Fig. 1. The mean and standard deviation of the intensities for the dependent dataset are 972.5 hPa and 24.9 hPa, and those for the independent dataset are 968.9 hPa and 26.5 hPa. The means obtained here are similar to the mean obtained by **?** using the operational aircraft reconnaissance measurements in 1980–1982 in the western North Pacific basin. This means that the collocated cases are representative. From Fig. 1, it can also be seen that the distribution of the independent dataset is more uniform, and the proportion for the strong intensity TCs in the latter is larger than that in the former, which means that the independent dataset will benefit the evaluation of robustness of the developed algorithm.

Additionally, limb darkening, which is the decrease in T_{B} with increasing scan angle for tropospheric sounding channels, and is caused by a longer slant path traveling through the absorbing atmosphere, should be considered. In order to maintain uniform sensitivity to a fixed atmospheric level across the full AMSU-A scan, a limb correction technique (**?**) must be implemented prior to the application of the measurements. For each channel and FOV, a limb-corrected T_{B} is produced using a weighted sum of the channel and its neighbors above and below. By using limb-corrected sounding channel T_{B}'s, the intensity estimation ensures that a channel remains sensitive to the temperatures at an almost constant level, regardless of scan angle.

3. A new algorithm for correcting effects of horizontal resolution

3.1 *AMSU-A observations of a tropical cyclone for different FOVs*

Because the horizontal resolution of AMSU-A cannot resolve the maximum warming, the observed peak warming is always less than the actual maximum value. Furthermore, the effect will vary with the size of the FOV, even for the same warm center. **?** investigated the effects of the coarse resolution of the MSU on the intensity estimation by a simulation study. Nowadays, due to NOAA-16 and NOAA-18 operating at the same time, it is possible to analyze the effects of the size of the FOV on warm anomaly observations for the same TC. The difference can be seen using the AMSU-A observations from NOAA-16 and NOAA-18 for the same cyclone. As shown in Fig. 2, two AMSU-A instruments onboard different satellites nearly contemporary observed the TC named NABI from the different local zenith angles. At almost

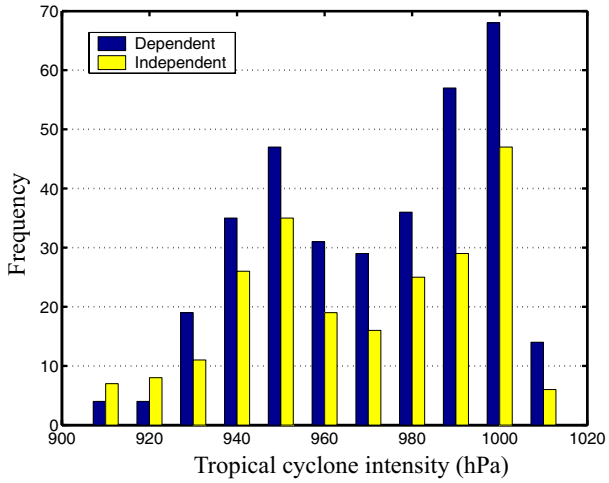

Fig. 1. Distribution of the collocated cases with the tropical cyclone intensity.

1700 UTC 31 August 2005, the TC eye is like a pinhole in the cloud image. The local zenith angles for the observations from two platforms are 57.9° and 5.7°. The corresponding FOV sizes are 150 km and 48 km respectively, and further analysis indicates that the relative difference of the T_{B} anomalies is over 40%. The difference is mainly caused by the following factors: the different horizontal resolution for the different scan geometries; and the relative position between the TC warm center and FOV. Due to difficulty in accurately defining the position of the cyclone center, here the authors focus on the effects of the first cause. The FOV size is 48 km in diameter at the near-nadir positions and grows gradually to about 150 km at positions 1 and 30. The variable FOV causes different measurements to be obtained for different areas, in which thermodynamic characteristics may be significantly non-uniform, especially for the FOV near the TC eye. Consequently, the horizontal resolution of the FOV has significant effects on the warm anomaly observation for the pinhole TC.

3.2 *Correction algorithm*

With the aim to decrease the effect of the variable horizontal resolution of AMSU-A on warm anomaly observations, a simple correction equation is developed. Observations show that the FOV size is a critical factor affecting anomaly observations. Additionally, Spencer and Braswell's (2001) study has shown that the T_{B} gradient near the TC center is related to TC intensity. The correction term may be simply related to the above two factors.

A correction algorithm, which is related to the product of the T_{B} gradient near the TC center and the size of the FOV observing the TC center, is proposed to modify the observed T_{B} of the FOV at the center. The corrected T_{B} is assumed as:

$$T_{\mathrm{B0}} = T_{\mathrm{B,obs1}} + k \cdot \frac{T_{\mathrm{B,obs1}} - T_{\mathrm{B,\ obs2}}}{R_0} \cdot R(\theta)\ , \qquad (1)$$

where the second term of the right-hand side of the

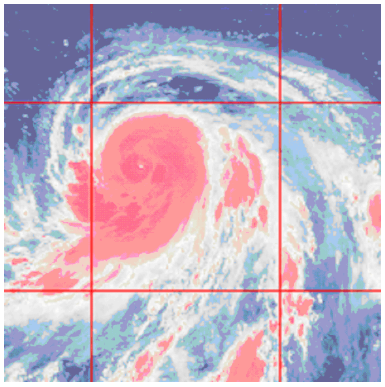

(a) Cloud image. 1630 UTC 31 August 2005.

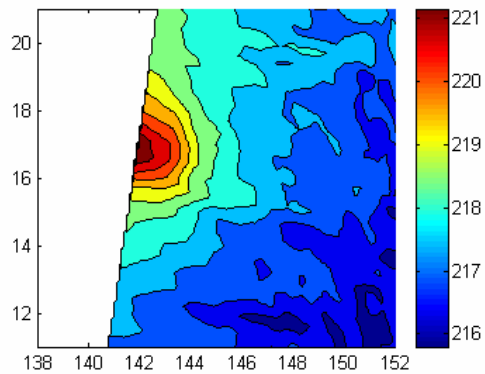

(b) Observation from NOAA-16. 1653 UTC 31 August 2005.

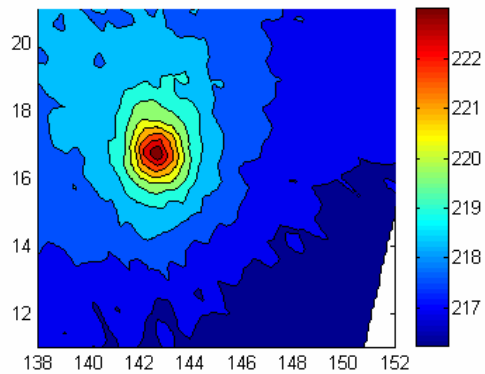

(c) Observation from NOAA-18. 1637 UTC 31 August 2005.

Fig. 2. Comparison of AMSU-A Ch8 observations of different FOVs for the same TC. (Typhoon is NABI; MSLP is 935 hPa from the BT data; position numbers of AMSU-A onboard NOAA-16 and NOAA-18 are 30 and 16).

Table 2. Relative differences (%) between the T_B's from NOAA-16 and NOAA-18 for different correction coefficients.

	$k = 0$	$k = 0.5$	$k = 1.0$	$k = 1.5$	$k = 2.0$	$k = 3.0$
Ch7	19	14	14	14	13	14
Ch8	17	12	9	9	10	10

equation is used to correct the effect of the varying size of the FOV on the TC center observation; $T_{B,obs1}$ is the measured T_B for the FOV at the TC center; $T_{B,\ obs1}$ is the measured T_B for the FOV next to the one observing the TC center; R_0=48 km; $(T_{B,obs1} - T_{B,\ obs2})/R_0$ can represent the gradient of the T_B in the along-track direction near the TC center; $R(\theta)$ is the variable horizontal resolution, which is related to the local zenith angle θ; and k is the correction coefficient and will be determined by the experiments using real observations. Although the correction equation is empirical in nature, the included physical meaning is that: the correction increases with the increase in the temperature gradient near the TC center and with the increase in the FOV size at the TC center. In order to verify the effectiveness of the proposed correction algorithm, the actual observations are applied to determine the correction coefficient and evaluate the algorithm in the following sections.

3.3 *Determination of the correction coefficient*

To develop and evaluate the correction algorithm, the data from NOAA-16 and NOAA-18 are collocated. From 1 July 2005 to 10 September 2005, the TCs HAITANG, MAWAR, TALIM, NABI, KHANUN occurred in the western North Pacific basin, and DENNIS, EMILY and KATRINA in the Atlantic basin, the intensities of which reached the category 4 level (Saffir-Simpson scale). There are 58 collocated cases available with the observations from NOAA-16 and NOAA-18 almost at the same time, the latitudes of which are lower than 40°N. It is likely that the level of maximum warming will vary in individual cases depending on latitude and environmental conditions. Furthermore, with the aim to decrease the effects of other factors on the development of the algorithm, only the cases with T_B anomalies exceeding 2.0 K at the 55.5-GHz channel are selected. Additionally, to guarantee that the gradient of T_B's near the TC center is large enough, the difference of the T_B's of the two adjoining FOVs should be larger than 1.0 K. For cases with large T_B anomalies, the small T_B gradient near the center may be caused by the fact that the TC center locates between the two adjoining FOVs, or is caused by the very large TC warm eye. Finally, 18 cases are obtained.

To determine the parameter and evaluate the correction algorithm, here the relative difference is defined as:

$$\frac{|\Delta T_{B18} - \Delta T_{B16}|}{\max[\Delta T_{B18}, \Delta T_{B16}]},$$

where ΔT_{B18} and ΔT_{B16} are T_B anomalies from NOAA-16 and NOAA-18 for the 54.94-GHz channel or the 55.5-GHz channel, and $\max[\Delta T_{B18}, \Delta T_{B16}]$ represents the maximum of the ΔT_{B18} and ΔT_{B16}.

To decrease the relative differences between the observations from NOAA-16 and NOAA-18 with different FOVs at the same TC center, the proposed correction algorithm is applied for different correction parameters in the experiments. Unfortunately, while the adjoining FOV observations in the along-track direction are used to calculate the T_B gradient near the TC center, the relative difference is not decreased as anticipated. The results may be caused by the fact that the center of the FOV is not the center of the actual warm center, which may fall between sensor beam positions or footprints. Furthermore, while the warm center is larger than the FOV, there may also be slight differences for the adjoining FOVs. To decrease the effects of the factors mentioned above, the FOV next to the adjoining one of the FOV measuring the TC center is applied in the experiments.

For the different values of k, six experiments were conducted. The results are given in Table 2. It is noted that the results using the 1.0 and 1.5 of k are better than those using the others. From Eq. (1), it is known that the larger the correction coefficient, the less the weight of the FOV measuring the TC center on the T_B's for the final estimation. Consequently, the smaller one is selected as the correction coefficient to emphasize the importance of the warmest FOV on the intensity estimation. For the available cases, the relative difference for the 55.5-GHz channel decreases from 17% to 9%. This means that the proposed algorithm can improve the level of the agreement between the T_B anomalies at the 54.94-GHz channel and the 55.5-GHz channel from NOAA-16 and NOAA-18. It is indicated that the correction algorithm can reduce the impacts of the different FOV sizes on observations.

Figure 3 shows the variations of the relative difference before and after the correction for the 18 cases. In this figure, $\mathrm{abs}(\theta_{18} - \theta_{16})$ is the absolute difference between the local zenith angles from NOAA-18 and NOAA-16. From Fig. 3, it can be seen that the rela-

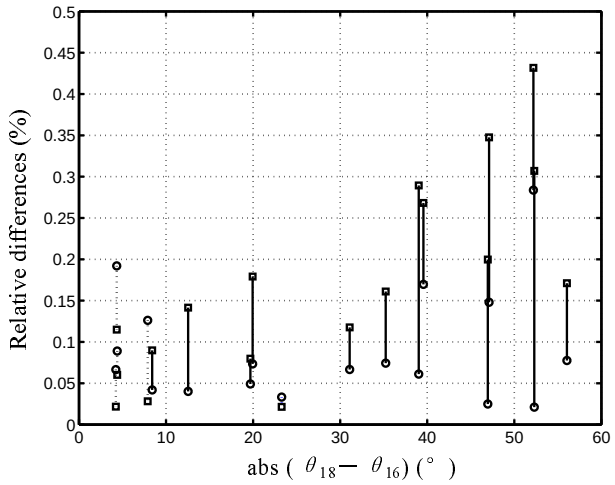

Fig. 3. Variation of the relative differences (%) before and after correction (rectangle—before correction; circle—after correction; solid line—decrease; dashed line—increase; $N = 18$; observation time differences of the two satellites are less than 2.5 h).

tive differences decrease for most cases with the local zenith angle difference larger than 10°. For the case shown in Fig. 2, the relative difference is decreased from 43% to 28%. For all cases, the correlation coefficient between the T_B anomalies from two different satellites is improved from 0.76 to 0.92 at the 55.5-GHz channel. These results suggest that the proposed correction algorithm can effectively reduce the effects of the different horizontal resolution on the T_B anomalies. However, for some cases with the local zenith angle difference less than 10°, the relative differences do not decrease, which is due to the fact that the effects caused by size differences of the FOVs are complicated with the effects caused by other factors, such as instrument noise, the intensity variation in the time difference between the observations by two platforms, scattering by large particles, and non-centering of the warm core region in the radiometer scan spot. Actually, it is very difficult to discriminate one of the above effects from the others.

3.4 *Validation and comparison with the physically-based correction method*

In this study, AMSU-A observations and BT data from the JMA are used to validate the correction algorithm. Furthermore, the physically-based scheme (**?**; **?**) is also used for comparison. In the physical scheme, the mean values from the climate statistics are used as the initial guesses. In the two schemes, due to no other measurements independent of AMSU-A being interpolated, the comparison is objective. The results are shown in Table 3. With the current correction algorithm, the correlation coefficients increase significantly at the 54.94-GHz channel and the 55.5-GHz channel for all cases. The increases mean that the new algorithm is effective. From Table 3, it is also indicated that the correction scheme obtains better results than the physically-based scheme. The results from the physical scheme are worse because it is significantly dependent on the initial conditions, especially for the size parameter. Obviously, the improvement of the correlation coefficients from our correction algorithm will benefit the performance of the intensity estimation using AMSU-A observations.

Additionally, it is shown that the correlation is significantly higher for the 55.5-GHz channel than for the 54.94-GHz channel. This is firstly because the actual peak warming in the TC may be occurring at levels higher than that sensed by the 54.94-GHz channel. Secondly, scattering by large particles may creep into the signal in very deep convection, resulting in a "cooling" of the radiances. Consequently, the 55.5-GHz channel can more accurately represent TC upper-tropospheric warming than the 54.94-GHz channel.

4. Estimation of TC intensity

4.1 *Development and validation of TC estimation scheme*

Assuming hydrostatic balance in the core region, a physical relationship should exist between the magnitude of the TC center warm temperature anomaly and the low pressure anomaly at the surface (Kidder et al., 1978). Using data from previous microwave instruments, several investigators have examined the relationship between temperature anomalies and the surface wind speed and central pressure of tropical cyclones (e.g., **??**; **?**; **?**; **?**). As shown in Table 3 and stated by **?**, there is a strong relationship between the T_B anomalies as measured by the AMSU-A instrument and TC intensity. The CIMSS (the Cooperative Institute for Meteorological Satellite Studies, University of Wisconsin-Madison) AMSU algorithm uses this relationship to estimate TC MSLP. In general, during the early stages of TC development the associated warm core is located near the 54.94-GHz channel, and that channel is used to produce an estimate. As the TC intensifies, the
warm core moves higher in the atmosphere, closer to the mean location of the 55.5-GHz channel. Experience indicates that once the TC reaches hurricane intensity the 55.5-GHz channel tends to be the better indicator of storm strength. Consequently, the algorithm in this study is based primarily on the 54.94-GHz channel and 55.5-GHz channel.

Table 3. Correlation coefficients between T_B anomalies and the BT intensity. (New—using the new correction scheme; Physical—using the physically-based scheme; Raw—no correction; N—the number of collocated cases).

Year	N	Ch7			Ch8		
		Raw	Physical	New	Raw	Physical	New
2002–2003	344	0.80	0.81	0.84	0.87	0.89	0.90
2004	229	0.83	0.82	0.85	0.88	0.90	0.92

Table 4. Comparison of different schemes of TC MSLP estimation. (Scheme A—with the new correction algorithm and the four channels; Scheme B—with the new correction algorithm and Ch7 and Ch8; Scheme C—only with Ch7 and without the new correction algorithm; CORR—correlation coefficient; RMSE—root mean square error; MAE—mean absolute error; BIAS—bias; STD—standard deviation of the differences between the estimated results and the best track intensities).

Scheme	Training					Validation				
	CORR	RMSE	MAE	BIAS	STD	CORR	RMSE	MAE	BIAS	STD
A	0.93	8.9	6.8	–	8.9	0.95	8.4	6.6	1.3	8.4
B	0.93	9.1	7.0	–	9.2	0.94	8.8	6.7	1.3	8.7
C	0.80	14.9	11.4	–	15.0	0.83	15.1	10.7	1.4	15.0

It is well known that scattering by wet ice and rain below the melting level overpowers the thermal signature. Even if the effects of horizontal resolution and viewing geometry can be accounted for, the problems of varying vertical structure of the warm anomaly and contamination of the thermal signature due to scattering by liquid water and wet ice remain (**?**). **?** included precipitation-sensitive channels as multiple regression predictors and **?** used AMSU cloud liquid water and cloud ice water correlation with reduced tropospheric sounding channel T_B to account for the scattering effect on the intensity estimation. Recently, in **?**, simulated AMSU T_B's were produced by a polarized reverse Monte Carlo radiative transfer model using representative TC precipitation profiles. The results suggest that precipitation depression of high-frequency window channel T_B's is correlated with depression of sounding channel T_B's and can be used to correct for scattering effects on the AMSU channels used in TC intensity estimates. Analysis of AMSU data over the tropical oceans confirms this and forms the basis for an empirical scattering correction using AMSU 31.4 and 89-GHz T_B's. This scattering correction reduces CIMSS TC MSLP algorithm RMS error by 10% in a 497 observation sample.

Based on the correction algorithm developed in the present study, a new scheme named A is proposed to estimate TC intensity. In this scheme, the T_B anomalies at 31.4 GHz and 89 GHz, which are used to take into account the effects of precipitation on estimation, are used directly as the predictors with those at 54.94 GHz and 55.5 GHz. Furthermore, due to the difference between the thermodynamic structures and scattering effects, two independent equations are developed for the weak and strong cyclones. The estimation equations are expressed as:

$$\begin{aligned}\text{MSLP} =& C_0 + C_1 \cdot \Delta T_{B7} + C_2 \cdot \Delta T_{B8} + \\ & C_3 \cdot \Delta T_{B15} + C_4 \cdot \Delta T_{B2}\end{aligned} \tag{2}$$

where MSLP is the estimated intensity; C_0, C_1, C_2, C_3, and C_4 are regression coefficients; and ΔT_{B7}, $\Delta T_{B8}, \Delta T_{B15}$ and ΔT_{B2} are T_B anomalies of channels 7, 8, 15 and 2. Figure 4 is a flowchart outlining the new algorithm. Multi-linear regression coefficients are obtained using the data from 2002–2003, and then the independent data from 2004 are used to validate the estimation equations. The statistical results are given in Table 4. The RMS difference of the validation results is 8.4 hPa and the correlation coefficient between the estimated results and the BT intensity data is 0.95. In comparison to the training case results, the results for validation are slightly better, likely signifying that there are a few cases with large errors.

Additionally, to evaluate the effects of the 31.4-GHz channel and 89-GHz channel on estimation, another scheme (named B) excluding their measurements is developed. The estimation results are also given in Table 4. Comparison of scheme A with scheme B indicates that measurements of the 31.4-GHz channel and 89-GHz channel can provide additional information on the estimation, the relative improvement of the RMSE from which is 5%. The coefficients of the regression equations for the A-method (including window channels) and B-method (excluding window channels), for

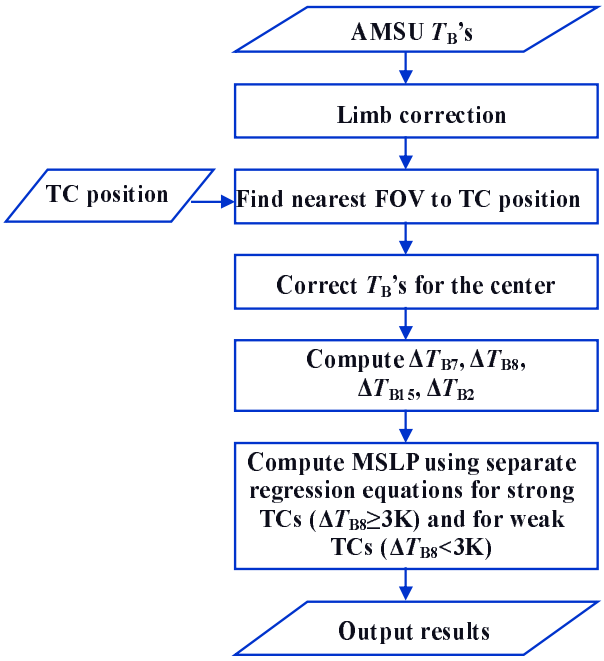

Fig. 4. Flowchart of AMSU-A-based TC intensity estimation algorithm.

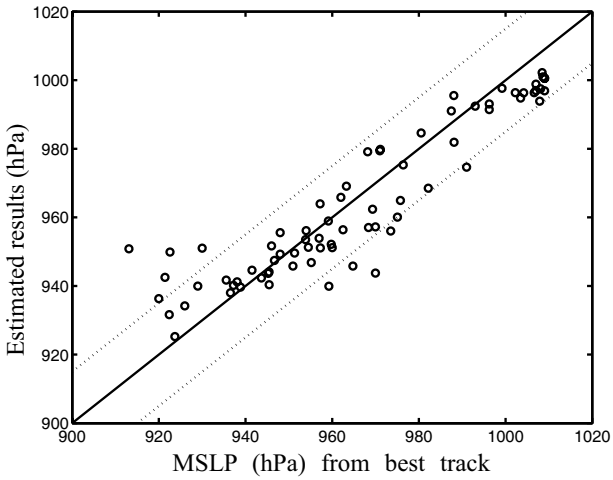

Fig. 5. Validation results of the developed algorithm using the collocated data over the Atlantic (solid line—true; dashed line—true±15 hPa; N = 74; RMSE=10.8 hPa; CORR=0.93).

both weak and intense hurricanes, are given in Table 5. Additionally, it is known that it may be partially clear in the FOV in the case of the warm core being smaller than the resolution, and it may be fully clear in the FOV in the case of the warm core being larger than the resolution. For the latter case, the warm anomaly is independent of large particles, which are usually in the eye wall. Due to the coarse resolution of AMSU-A, the data from other instruments are needed for separating the above two cases. For more effectively using the two channels, a physical scheme will be studied in the near future.

? developed an MSLP estimation technique at CIMSS using AMSU-A 54.94-GHz channel T_B anomalies, along with Merrill's (1995) physically-based warm anomaly retrieval scheme. In their study, Automated Tropical Cyclone Forecast eye size information was incorporated, which improved the performance of the MSLP estimates with mean error and standard deviations. Compared to the scheme using raw AMSU-A 54.94-GHz UTWA observations alone, the relative improvements of the RMSE and the standard deviation of the error were also 27% for the collocated data in 2000.

Similar to other studies (**?**; **?**), a scheme C, as used in Brueske and Velden's (2003) study, which only uses the temperature anomaly at the 54.94-GHz channel and does not apply the present correction algorithm, is developed. The results are shown in Table 4. It is noted that the results of scheme A are significantly better than those of scheme C. The relative improvements of RMSE and standard deviation of the error are 39% and 44% (see Table 4). Obviously, it is not possible to obtain enough accurate results for all cases only by using the 54.94-GHz channel. The above comparisons indicate that the new scheme is effective for estimating MSLP from AMSU-A data. At the same time, due to no other information independent of AMSU-A being included, the implementation of the scheme may be more feasible for operational application.

4.2 *Evaluation of the developed algorithm using Atlantic cases*

To further evaluate AMSU estimation of TC intensity, the developed algorithm is applied using Atlantic basin collocated data from 2004. Due to long term operational reconnaissance observations performed by the National Hurricane Center (NHC) in the Atlantic basin, which make substantial contributions to the BT data, the data can be considered as approaching the "truth". TCs that reached the category 2 level were selected to evaluate the algorithm, which include: FABIAN, ISABEL, JUAN, KATE, ALEX, CHARLEY, DANIELLE, FRANCES, IVAN, JEANNE, and KARL. There were 74 cases available, the mean and standard deviation of which are 965.8 hPa and 27.4 hPa, respectively. Compared to the collocated data in the above sections, the intensities are stronger and more disperse. Consequently, they are more effective for evaluating the robustness of the developed algorithm. The relationship between estimated results and the BT data is shown in Fig. 5.

Table 5. TC MSLP estimation coefficients using Schemes A and B.

Scheme		C_0	C_1	C_2	C_3	C_4
A	$\Delta T_{B8} \geqslant 3$ K	977.7258	1.9322	−6.4594	0.0273	−0.0266
	$\Delta T_{B8} < 3$ K	1002.3326	−8.3246	−0.6916	0.1570	−0.0528
B	$\Delta T_{B8} \geqslant 3$ K	975.9715	3.0739	−7.5818	–	–
	$\Delta T_{B8} <3$ K	1001.8123	−4.6076	−5.2684	–	–

Table 6. Statistical results of the estimated TC intensities by using the new scheme and the CIMSS AMSU products against the BT intensity data in the western North Pacific (WP) and Atlantic (AL) basins.

	WP; Jun.–Dec. 2004; N=81					AL; Aug.–Sep. 2004; N=24				
	CORR	RMSE	MAE	BIAS	STD	CORR	RMSE	MAE	BIAS	STD
New	0.95	8.7	7.0	0.9	8.9	0.94	9.0	7.2	3.3	8.5
CIMSS	0.94	10.2	7.6	−0.5	10.4	0.94	9.5	7.7	1.2	9.5

The correlation coefficient between the above data is 0.93. The root mean square difference is 10.8 hPa and the bias is −1.6 hPa. These results demonstrate that the developed algorithm is robust. **?** showed that the results of 288 cases with BT data in the Atlantic basin produced a RMSE of 10.5 hPa and a bias of −1.1 hPa. These results suggest that the developed algorithm, which only depends on AMSU-A data, can provide intensity estimates that are comparable to Demuth et al.'s (2004) algorithm.

While the developed regression equation is used for Atlantic cases, significant underestimates are found for some strong cases in Fig. 5. The major reason for this is the basic structural differences in the thermal anomalies and environments between Atlantic hurricanes and western North Pacific typhoons. As Merrill's (1984) study showed, the mean typhoon is twice as large in area as the mean hurricane. When the scheme is redeveloped for Atlantic cases, more accurate results are expected.

4.3 *Comparison with CIMSS AMSU products*

The CIMSS AMSU algorithm also uses the T_B anomalies at the 54.94-GHz channel and 55.5-GHz channel to estimate TC MSLP. One of the main differences between the developed method here and the CIMSS algorithm is that the latter use other data independent of AMSU measurements to account for the effects of subsampling. In the CIMSS estimation algorithm, the regression coefficients are developed using data from 1998–2003. For more details of the CIMSS algorithm, see the CIMSS website (http://amsu.ssec.wisc.edu/explanation.html). The CIMSS products were downloaded from the above site before April 2006.

After the available collocated cases in 2004 in the western North Pacific and Atlantic basins are matched again with the available CIMSS products, we obtain 81 and 24 collocated cases respectively for the above two basins. The statistical results are given in Table 6. For the western North Pacific and Atlantic cases, the standard deviation of the differences of the results compared to the CIMSS products are 15% and 11% less, respectively. The results indicate that consistency between the estimation results and the BT data are better. In the western North Pacific basin, the lower difference between the results and the BT data are obtained mainly because the testing cases and the training cases are from the same area. However, it is also noted that the results in comparison to the CIMSS products are better even for the collocated data in the Atlantic basin, which are fully independent of the training data. The above results indicate that the developed estimation algorithm is reliable. Additionally, it is found that there is a significant bias when the estimation algorithm obtained from the collocated data over the western North Pacific basin are applied to estimate TC intensity in the Atlantic basin, which is due to the fact that the distributions of TC size and intensity are different for different basins, as mentioned in section 4.2.

4.4 *Error analysis*

In this study, the BT data are used to develop and validate the algorithm. Because they are not all "ground truths", uncertainty in the BT intensity data is one of the major causes of the final differences. Particularly for the western North Pacific basin data, there are no operational aircraft reconnaissance measurements to be incorporated into the BT data.

Merrill (1995) investigated the effects of some factors on the microwave TC intensity estimation by using simulation studies. In the present study, observations show that in the case of a small TC eye, there are great effects on the T_B observation due to the coarse and variable resolution of AMSU-A. Although some

improvement has been obtained for the agreement between observations from the instruments onboard two different satellites by using the developed correction algorithm, the coarse and variable resolution is still a significant influencing factor on the error. Furthermore, interactions between the varying weighting function shapes and heights and the warm anomaly are not accounted for by limb correction. Additionally, the cases in which the actual hurricane's eye is outside the warmest FOV are not considered. These factors all decrease the effective accuracy of the observations. Other known factors, including radiometer noise, nonconstant environmental pressure, non-centering of the warm core region in the radiometer scan spot, and the weighting function not peaking at the level of maximum temperature anomaly, are all causes of variance in the estimation results.

5. Summary and conclusions

In this study, AMSU-A measurements have been used to estimate TC intensity. The observations from different satellites have shown that the variable horizontal resolution of the instrument has significant effects on the sensitivity of the T_{B} anomalies. In order to reduce the effects on TC intensity estimation more easily and effectively, a new correction algorithm has been proposed to modify the observed T_{B} anomalies. After applying and evaluating the correction algorithm for cases over the western North Pacific from 2002–2004, it have been shown that the algorithm can significantly improve the correlation between T_{B} anomalies at the 54.94-GHz channel and 55.5-GHz channel and the BT intensity, and has the potential to improve the accuracy of AMSU TC intensity estimation. Furthermore, the T_{B} anomalies at 31.4 GHz and 89 GHz, which were used to take into account the effects of precipitation on estimation, were directly as the predictors with those at 54.94 GHz and 55.5 GHz to develop the regression algorithm in the western North Pacific basin. Without the parameters obtained from other measurements, the algorithm yielded 8.4 hPa of the RMS error and 6.6 hPa of the mean absolute error for 229 independent cases. Additionally, a further evaluation of the constructed regression algorithm was performed for the cases with coincident NHC post-analyzed BT data in the Atlantic basin. The results were reasonable, although there was a significant bias, especially for some strong cases. Finally, a preliminary comparison with CIMSS AMSU products suggested that the performance of the new scheme appears to be better for the available cases.

Although this study has primarily focused on the western North Pacific, the estimation scheme as shown in Fig. 4 can be run in other tropical basins to obtain basin-dependent TC MSLP estimation coefficients. When a sufficient number of AMSU cases with coincident reconnaissance data are available, the intensity algorithm may be redeveloped so that they are based entirely on "ground truths", making them completely independent of the BT data. Additionally, how to obtain the correction coefficient is a very important issue. In this study, it was determined by decreasing the relative differences between the collocated measurements from NOAA-16 and NOAA-18. If no collocated data are available from the instruments onboard different satellites, an alternative way would be to maximize the correlation coefficient between AMSU-A measurements and coincident reconnaissance data, or the BT intensity data. In the near future, except for augmenting the training dataset, other measurements with higher horizontal resolution, such as AMSU-B, may be included to further enhance the capability of estimating TC intensity using microwave data.

Acknowledgements. The authors would like to thank NOAA/NESDIS for providing the AMSU-A data, the JMA and NOAA/NHC for providing the best track data, CIMSS for providing TC intensity AMSU estimation products, Dr. Z. Han for useful discussions, and Mr. L. Wang for assistance with data acquisition. The two anonymous reviewers' comments were of considerable help in improving the text and clarifying the issues. This research was funded by the Major State Basic Research Development Program of China (Grant No. 2001CB309402).

REFERENCES

Brueske, K. F., and C. S. Velden, 2003: Satellite-based tropical cyclone intensity estimation using NOAA-KLM series Advanced Microwave Sounding Unit (AMSU) data. *Mon. Wea. Rev.*, **131**, 687–697.

Demuth, J. L., M. Demaria, J. A. Knaff, and T. H. Vonder Haar, 2004: Evaluation of Advanced Microwave Sounding Unit tropical-cyclone intensity and size estimation algorithms. *J. Appl. Meteor.*, **43**, 282–296.

Goldberg, M. D., D. S. Crosby, and L. Zhou, 2001: The limb adjustment AMSU-A observations: Methodology and validation. *J. Appl. Meteor.*, **40**, 70–83.

Kidder, S. Q., W. M. Gray, and T. H. Vonder Haar, 1978: Estimating tropical cyclone central pressure and outer winds from satellite microwave data. *Mon. Wea. Rev.*, **106**, 1458–1464.

Kidder, S. Q., W. M. Gray, and T. H. Vonder Haar, 1980: Tropical cyclone outer surface winds derived from satellite microwave sounder data. *Mon. Wea. Rev.*, **108**, 144–152.

Kidder, S. Q., M. D. Goldberg, and R. M. Zehr, M. DeMaria, J. F. W. Purdom, C. S. Velden, N. C. Grody, and S. J. Kusselson, 2000: Satellite analysis of tropi-

cal cyclones using the advanced microwave sounding unit (AMSU). *Bull. Amer. Meteor. Soc.*, **81**, 1241–1259.

Merrill, R. T., 1984: A comparison of large and small tropical cyclones. *Mon. Wea. Rev.*, **112**, 1408–1418.

Merrill, R. T., 1995: Simulations of physical retrieval of tropical cyclone thermal structure using 55-GHz band passive microwave observations from polar-orbiting satellites. *J. Appl. Meteor.*, **34**, 773–787.

Qiu, H., S. Gu, Y. Zhu, W. Zhang, and X. Fang, 2004: Estimation of the central surface pressure of tropical cyclone from satellite microwave data. *Chinese Journal of Radio Science*, **19**, 393–398. (in Chinese)

Spencer, R. W., and W. D. Braswell, 2001: Atlantic tropical cyclone monitoring with AMSU-A: Estimation of maximum sustained wind speeds. *Mon. Wea. Rev.*, **129**, 1519–1532.

Velden, C. S., 1989: Observational analyses of North Atlantic tropical cyclones from NOAA Polar-Orbiting Satellite Microwave data. *J. Appl. Meteor.*, **28**, 59–70.

Velden, C. S., and W. L. Smith, 1983: Monitoring tropical cyclone evolution with NOAA satellite microwave observations. *J. Appl. Meteor.*, **22**, 714–724.

Velden, C. S., B. M. Goodman, and R. T. Merrill, 1991: Western North Pacific tropical cyclone intensity estimation from NOAA polar-orbiting satellite microwave data. *Mon. Wea. Rev.*, **119**, 159–168.

Velden, C. S., T. L. Olander, and R. M. Zehr, 1998: Development of an objective scheme to estimate tropical cyclone intensity from digital geostationary satellite infrared imagery. *Wea. Forecasting*, **13**, 172–186.

Wacker, R. S., 2005: Correcting for precipitation effects in satellite-based passive microwave tropical cyclone intensity estimates. Ph. D. Dissertation, University of Wisconsin-Madison, 146pp.

Weatherford, C., and W. M. Gray, 1988: Typhoon structure as revealed by aircraft reconnaissance. Part I: Data Analysis and Climatology. *Mon. Wea. Rev.*, **116**, 1032–1043.